Mem. Fac. Sci.
Kochi Univ.
(Inform. Sci.)
15 (1994), 131–142

SCALE DEPENDENCE OF THE FRACTAL DIMENSION OF ATMOSPHERIC VARIABILITY

Takahiro IWAYAMA[1], Takahiro KAYAHARA[1], Hisao OKAMOTO[2] and Michiya URYU[1*)]

[1] Department of Physics, Faculty of Science, Kyushu University, Fukuoka 812, Japan.
[2] Department of Information Science, Faculty of Science, Kochi University, Kochi 780, Japan.

(Received November 26, 1993)

Abstract

In the present work, a fractal analysis is performed for 500mb geopotential height obtained from FGGE III b data set. The fractal dimension evaluated in the present work represents the dimension of the set of points $(t, Z(t))$, where t is time and $Z(t)$ is the geopotential height. Depending on the sampling time of the time series, the fractal dimension D has a different value. When the sampling time k is less than $k_1 (\approx 3$ days), $D = 1.3 \sim 1.5$. As $k_1 < k < k_2 (= 30 \sim 40$ days), $D \approx 1.9$. When $k > k_2$, $D \approx 1.6$. These time scales indicate specifically the synoptic scale phenomena, the planetary scale phenomena and the semiannual and the annual variabilities, respectively. Moreover, the local dispersion is introduced and is applied to the data. The results of the local dispersion analysis coincide with those of the fractal dimension analysis. Although the fractal dimension evaluated in this work does not directly represent the numbers of independent variables of dynamical system, the results imply that the number of the independent variables that describe the atmospheric phenomena has different value depending on the scale of interest.

1. Introduction

It can be considered that the number of independent variables that describe atmospheric phenomena depends on a scale of interest, because dominant terms of the atmospheric governing equations depend on the scale. In addition, a fractal dimension of an attractor of a time series, e.g., the correlation dimension, represents the number of independent variables of the system. Thus we investigate what the scale dependence of the fractal dimensions of the atmospheric attractor is.

*) He went to his final rest in Aug. 1990.

After the work of Nicolis and Nicolis [1], many works to estimate the correlation dimension of the weather and the climate attractors have been performed [2–6]. However, the existence of the low-dimensional weather and climate attractors has been distrusted, recently. It has been pointed out that there is the possibility of evaluating false low-dimension from less number of data [7, 8]. The relation between the number of data and the reliability of evaluated correlation dimension is discussed by some authors [9–11].

In the present work, a fractal dimension of geometry of a time series is evaluated, because the existence of low-dimensional weather and climate attractors has been distrusted. The fractal dimension evaluated in the present work represents the dimension of the set of points $(t, Z(t))$, where t is time and $Z(t)$ is a physical quantity, e.g., the geopotential height. Thus the fractal dimension does not represent the number of the independent variables. Nevertheless, we infer that there exists a scale dependence in the variability of time series, i.e., the scale dependence of the fractal dimension is introduced and is evaluated in the preset work.

In the present work, the fractal dimensions of an annual time series of 500mb geopotential height, located at 60° and 30° of both the northern and the southern latitudes and the equator, are evaluated. The data is obtained from FGGE[1] III b data sets (main III b produced by GFDL[2]). The interval of the data is a half day.

Yano and Nishi [12] performed a fractal analysis for NOAA[3] OLR[4] data, in order to see a clear scale separation in the variability of the tropical atmosphere. The calculation method they used is one which measures the change of variability as the period of averaging of data is changed. Moreover the advantage of the method is to measure directly the change of the fractal dimension depending on a time scale.

In the present work, the fractal dimension is evaluated by using a method proposed by Higuchi [13]. The method has the advantage of which the fractal dimension can accurately be evaluated even for small number of data. We do not have much data, (the length of the data set is 730 for each grid point), hence we use the method proposed by him. We must pay attention to the interpretation of results, because Yano and Nishi [12] said that the method was not sensitive to the presence of scale-separation. Thus we introduce the local dispersion, that is similar to the method used by them.

[1] First Global atmospheric research programme Global Experiment.
[2] Geophysical Fluid Dynamics Laboratory.
[3] National Oceanic and Atmospheric Administration.
[4] Outgoing Long Wave Radiation.

and apply it to the data.

The idea of the scale dependence of the fractal dimension is similar but not to that of the multifractal [14]. The multifractal refers to the non-uniformity of the attractor and to the existence of the intinite numbers of fractal dimension. However, the scale dependence of the fractal dimension of the attractor refers to that the different value of the fractal dimension is evaluated if the extent of the coarse graining scale is changed.

2. Methods for data analyses

2.1 Fractal dimension

There are many methods to calculate the fractal dimension. In the present work, we use a method proposed by Higuchi [13]. This is a modification of Burlaga and Klein's method [15]. In the method, the fractal dimension represents the dimension of the set of points $(t, Z(t))$, where t is time and $Z(t)$ is a physical quantity, e.g., the geopotential height. Thus it is the geometrical measure to classify the curve of $(t, Z(t))$, quanitiatively. The calculation method is described in the following.

A new time series X_m^k is constructed from a given time series $\{X_i;\ i = 1, 2, \ldots, N\}$ as follows,

$$X_m^k;\ X_m,\ X_{m+k},\ X_{m+2k}, \ldots, X_{m+\left[\frac{N-m}{k}\right]k}, \tag{2.1}$$

where m represents the initial time, k is the sampling time and $[\cdots]$ denotes the Gauss' notation. Next the length $L_m(k)$ of the curve X_m^k is defined as follows,

$$L_m(k) \equiv \left\{ \frac{N-1}{\left[\frac{N-m}{k}\right] \cdot k} \left(\sum_{i=1}^{\left[\frac{N-m}{k}\right]} |X_{m+i\cdot k} - X_{m+(i-1)\cdot k}| \right) \right\} / k. \tag{2.2}$$

If the average of $L_m(k)$ over m, say $L(k)$, satisfies the following relation, D is called the fractal dimension:

$$L(k) \sim k^{-D}. \tag{2.3}$$

If the time series has the character similar to the fractal Brownian motion, its power spectrum obeys a power law:

$$P(\omega) \sim \omega^{-\alpha} \tag{2.4}$$

and the exponent α is related to the fractal dimension D by

$$D = \frac{5 - \alpha}{2}. \tag{2.5}$$

The method has an advantage that the fractal dimension can be accurately evaluated even for small number of data. However, we must pay attention to the interpretation of results, because Yano and Nishi [12] stated that the method was not sensitive to the presence of the scale-separation.

2.2 Local dispersion

The local dispersion is introduced in this subsection. This is similar to the fractal dimension used by Yano and Nishi [12].

A new time series $M_{L,i}$ is constructed from the running mean of a given time series $\{X_i;\ i = 1, 2, \ldots\}$ as follows:

$$M_{L,i} \equiv \frac{1}{L} \sum_{j=0}^{L-1} X_{i+j}, \tag{2.6}$$

where L is the averaging time. Using this time series, local dispersion σ_L is defined as follows:

$$\sigma_L \equiv \langle (X_i - M_{L,i})^2 \rangle \tag{2.7}$$

where $\langle \cdots \rangle$ denotes the average over the initial time i. It is convenient to normalize σ_L by the ordinary dispersion $\sigma (= \sigma_{L=\infty})$. Hereafter, the local dispersion σ_L refers to one which is normalized by σ.

If the time series $\{X_i\}$ have the ergodic property, σ_L can be related to the autocorrelation coefficient $\phi(\tau)$,

$$\sigma_L = \frac{L-1}{L} - \frac{2}{L^2} \sum_{\tau=1}^{L-1} \tau \cdot \phi(\tau), \tag{2.8}$$

where

$$\phi(\tau) = \frac{\langle (X_i X_{i+\tau}) \rangle}{\langle X_i^2 \rangle}. \tag{2.9}$$

For continuous data $X(t)$, the running mean and the local dispersion $\sigma(L)$ are similarly defined:

$$M(L; t) \equiv \frac{1}{L} \int_t^{t+L} X(t')dt', \tag{2.10}$$

$$\sigma(L) \equiv \langle (X(t) - M(L; t))^2 \rangle. \tag{2.11}$$

If the time series are ergodic, the following relation holds:

$$\sigma(L) = 1 - \frac{2}{L^2}\int_0^L \tau \cdot \phi(\tau) d\tau, \tag{2.12}$$

where $\sigma(L)$ has been also normalized by $\sigma(=\sigma(\infty))$.

Two simple examples of the local dispersion are given in the following. For a random time series,

$$\phi(\tau) = \delta_{\tau,0}, \tag{2.13}$$

we obtain

$$\sigma_L = \frac{L-1}{L}. \tag{2.14}$$

Thus the local dispersion σ_L is concave for any $L(L>1)$.

As another example, for sinusoidal time series,

$$\phi(\tau) = \cos\tau, \tag{2.15}$$

we obtain

$$\sigma(L) = \frac{L^2+2}{L^2} - \frac{2(L\sin L + \cos L)}{L^2}. \tag{2.16}$$

If L is small enough to satisfy the following expansions,

$$\sin L \approx L - \frac{1}{3!}L^3,$$

$$\cos L \approx 1 - \frac{1}{2!}L^2 + \frac{1}{4!}L^4,$$

(2.16) becomes

$$\sigma(L) = \frac{L^2}{4} + O(L^4). \tag{2.17}$$

Thus $\sigma(L)$ is convex for $0 < L \ll 1$. Hence the average time at which σ_L (or $\sigma(L)$) has the inflection point corresponds to the time scale at which the statistical regularity of time series changes.

The local dispersion is related to the correlation coefficient by (2.8) and (2.12), and the correlation coefficient is related to the power spectrum through the Fourier transformation. Moreover the slope of the power spectrum is related to the fractal dimension D by (2.5). Thus the change of D may be detected by the analysis of the local dispersion. The direct relationship

between the change of D and σ_L (or $\sigma(L)$) has not known yet. However in this article it is inferred that the time at which σ_L (or $\sigma(L)$) has inflection point relates the time scale at which D changes its value.

3. Results and Discussion

3.1 Data

In the present work, the annual time series of 500mb geopotential height, $Z(t)$, obtained from FGGE III b data sets (main III b produced by GFDL), are analyzed. The data set is constructed from the annually (from Dec. 1st, 1978 to Nov. 30th, 1979) observed meteorological elements on the grid points with the longitudinal and the latitudinal resolution $\Delta\lambda \times \Delta\phi = 1.875^\circ \times 1.875^\circ$, respectively. The time interval of the data is a half day. Thus there are 192 grid points on a latitudinal circle and the total number of data for each grid point is 730.

3.2 The fractal dimension

We firstly show the results of the fractal dimension analyses. The lengths $L(k)$, mentioned is Sec. 2.1, are evaluated for each grid points on the latitudinal circles of 60°N, 30°N, 0°(EQ), 30°S and 60°S. The results are shown for the value averaged over all grid points on each latitudinal circle, i.e., zonally averaged value.

Figure 1 show the relation between the sampling time k of newly constructed time series X_m^k and $L(k)$ defined by (2.2). The slope of the curve in the figure represents the value of the fractal dimension D. The fractal dimension D changes its value at the sampling time $k_1 (\sim 3$ days) except for EQ. Moreover, it also changes at $k_2 (= 30 \sim 40$ days) for 60°N and 30°N. The values of D and the sampling time at which D changes its value are listed in Table I and Table II, respectively.

The phenomena with a longer period than $2k$ are included in the time series provided that the sampling time of the time series is k. Hence the synoptic scale phenomena may be realized in the time series which the sampling time $k < k_1$. Planetary scale flows may be realized in those with the sampling time k, $k_1 < k < k_2$, because the long term variabilities (oscillations having periods longer than 10 days) are contained in the planetary modes [16, 17]. A semiannual or an annual variability may be realized in those with the sampling time $k > k_2$.

The time series with sampling time k, $k_1 < k < k_2$, are similar to a random noise, because the fractal dimension of the time series in this sampling time is nearly equal to that of a random noise, that has $D = 2$. Thus it implies

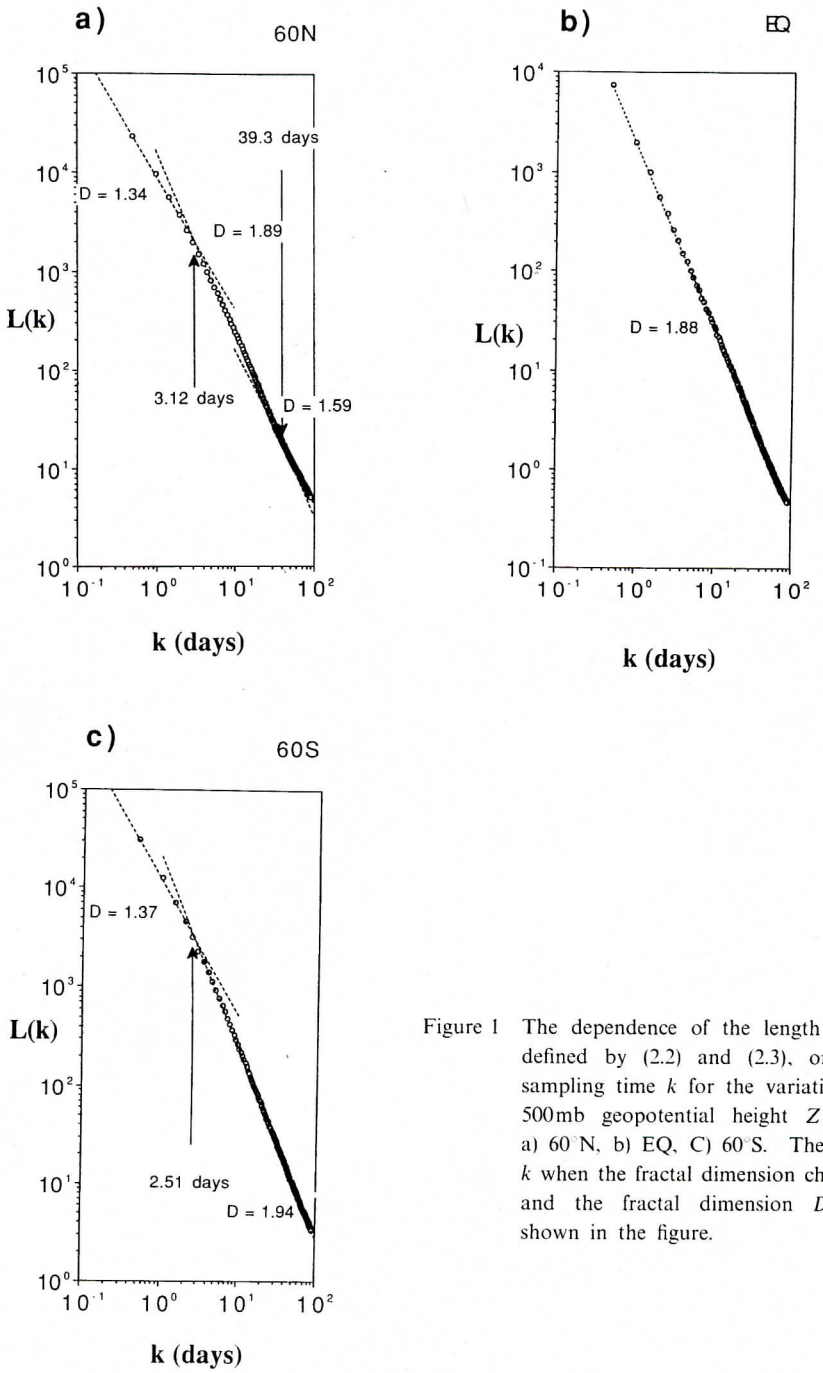

Figure 1 The dependence of the length $L(k)$, defined by (2.2) and (2.3), on the sampling time k for the variation of 500mb geopotential height $Z(t)$ at a) 60°N, b) EQ, C) 60°S. The time k when the fractal dimension changes and the fractal dimension D are shown in the figure.

Table I. The sampling time at which the fractal dimension changes its value. Unit is days.

	60°N	30°N	EQ	30°S	60°S
k_1	3.12	3.49		2.76	2.51
k_2	39.3	33.3			

Table II. The values of the fractal dimension D.

	60°N	30°N	EQ	30°S	60°S
$k < k_1$	1.34	1.56		1.43	1.37
$k_1 < k < k_2$	1.89	1.89	1.88	1.88	1.94
$k_2 < k$	1.59	1.64			

that the phenomena are unpredictable in this time scale. This is supported by the results of Egger and Schilling [17, 18]. They stated that planetary scale flows, that contained the long term variability, were induced by the stochastic forcing of the synoptic scale flows, hence the long term variabilities were unpredictable.

The synoptic scale phenomena can be predicted in the frame work of the baroclinic instability theory [19, 20]. Moreover semiannual and annual oscillations are predictable, because those synchronize with the sun. Thus the phenomena realized in the time series with the sampling time k, $k < k_1$ and $k > k_2$, are predictable compared with those with $k_1 < k < k_2$. The reasons of the nonexistence of the time k_2 in the southern hemisphere are considered later on.

For EQ, there does not exist any time scale as k_1 and k_2 within time interval less than 90 days and we obtain $D = 1.88$, i.e., the graph of the time series, $(t, Z(t))$, for EQ has a uniform fractal structure within time interval less than 90 days.

3.2. local dispersion

The local dispersion σ_L, introduced in Sec. 2.2, are evaluated at 60°N, EQ and 60°S on 127.5°E, (see Fig. 2). Let the averaging time at which the curvature of σ_L changes from convex to concave be L_1 and the averaging time at which the curvature of σ_L changes from concave to convex be L_2. At 60°N, 30°N, 30°S and 60°S, $L_1 \sim 1$ day and $L_2 = 10 \sim 15$ days. On the other hand EQ, $L_2 \sim 30$ days and L_1 does not exist within less than 30 days, (L_1 and L_2 are tabulated in Table III.). This inflection point of σ_L is equivalent to the scale-separation time that Yano and Nishi [12] stated. Hence, L_1 and L_2 correspond to k_1 and k_2, respectively, and the sampling time at which D changes its value may exist two, k_1 and k_2, at 60°N, 30°N, 30°S and 60°S, and 60°S, and one, k_2, at EQ. The difference between the values of k_1 and L_1 and those of k_2 and L_2 may come from their definitions: k is the sampling time but L is the averaging time.

The curvature of σ_L is convex if an average time L is $L < L_1$ or

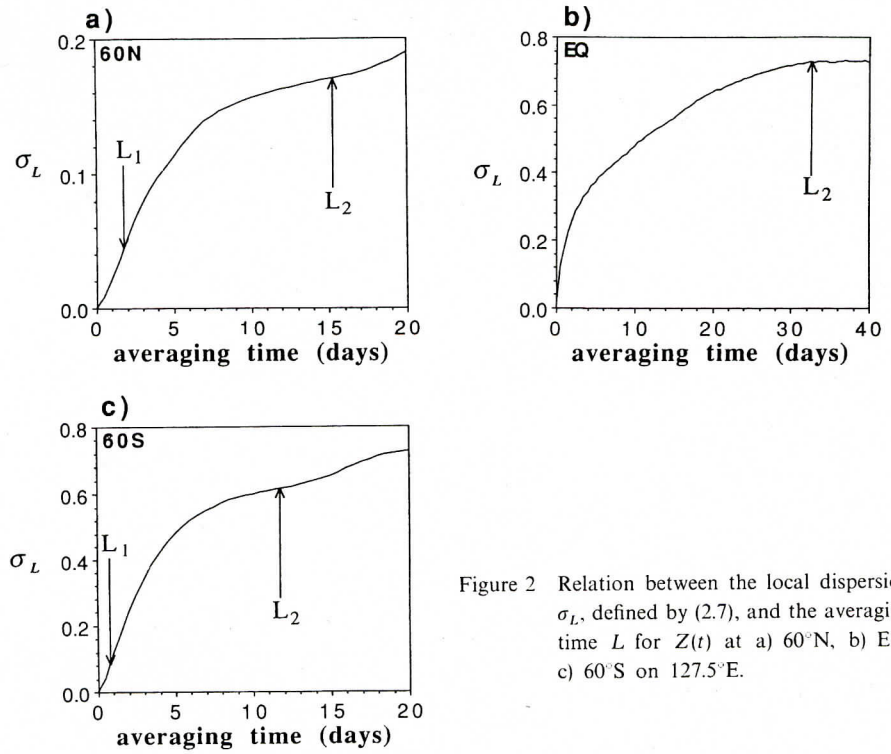

Figure 2 Relation between the local dispersion σ_L, defined by (2.7), and the averaging time L for $Z(t)$ at a) 60°N, b) EQ, c) 60°S on 127.5°E.

Table III. The averaging time at which the local dispersion σ_L of $Z(t)$ has the inflection point. Unit is days.

	60°N	30°N	EQ	30°S	60°S
L_1	1.75	1.25		1.25	0.75
L_2	15.25	14.75	32.75	12.25	11.75

$L > L_2$. Thus the time series are statistically regular just as sinusoidal curve, provided that the averaging time L is $L < L_1$ or $L > L_2$. On the other hand, the curvature of σ_L is concave if L is $L_1 < L < L_2$. Thus the time series are statistically irregular just as random noise, provided that L is $L_1 < L < L_2$. These coincide with the results of fractal dimension analyses, stated in sec. 3.1.

Here, we consider the nonexistence of k_2 in the southern hemisphere and the equator. We construct new time series $M(L_2; t)$ that are produced by taking the running mean with an averaging time L_2 from $Z(t)$, and $Z'(L_2; t)(\equiv Z(t) - M(L_2; t))$. The standard deviations of $M(L_2; t)$ and

$Z'(L_2; t)$ are shown in Fig. 3. In the southern hemisphere and the equator the standard deviations of $M(L_2; t)$ and $Z'(L_2; t)$ are nearly equal. We can consider that $M(L_2; t)$ and $Z'(L_2; t)$ are the planetary scale variability and the synoptic scale variability, respectively. Thus, figure 3 represents the weakness of the activities of planetary scale waves in the southern hemisphere and the equator. It is actually known that the activities of planetary scale waves are weak in the southern hemisphere [21]. Thus the reason of the nonexistence of k_2 in the southern hemisphere and the equator is reduced to the weakness of the activities of planetary waves. Moreover, it is suggested that the calculation method proposed by Higuchi [13] does not work sensitively to extract the existence of the scale separation, as Yano and Nishi [12] have stated.

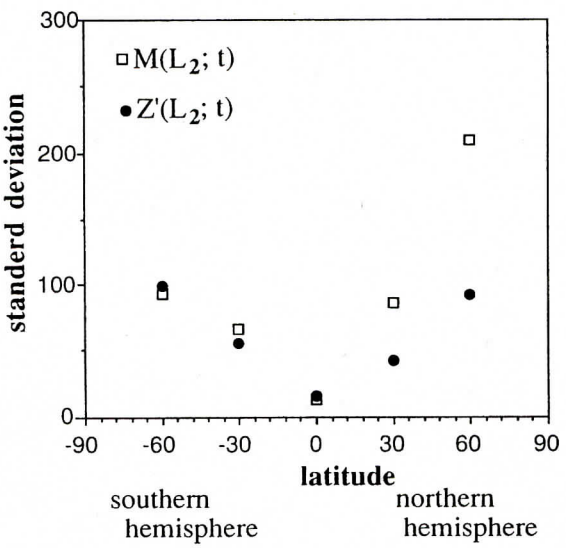

Figure 3 Dependence of the standard deviation of data $M(L_2; t)$ and $Z'(L_2; t)$ on each latitude, where $M(L_2; t)$ is the time series produced by running mean with averaging time L_2 from $Z(t)$, and $Z'(L_2; t) = Z(t) - M(L_2; t)$.

4. Concluding remarks

In the present work, a fractal analysis was performed for 500mb geopotential height, located at 60°N, 30°N, 0°(EQ), 30°S and 60°S, obtained from FGGE III b data set. The fractal dimension evaluated in the present work was the one which has been proposed by Higuchi [13] and represents the dimension of the set of points $(t, Z(t))$, where t is the time and $Z(t)$ is

the geopotential height. Depending on the sampling time of the time series, the fractal dimension D takes different value. When the sampling time k was less than $k_1 (\approx 3$ days), it took $D = 1.3 \sim 1.5$. As the sampling time k was greater than k_1 and less than $k_2 (= 30 \sim 40$ darys), $D \approx 1.9$. When the sampling time k was greater than k_2, $D \approx 1.6$. These time scales indicated specifically the synoptic scale phenomena, the planetary scale phenomena and the semiannual and annual variability, respectively. Moreover, the local dispersion, that was similar to the fractal dimension used by Yano and Nishi [12], was introduced and was applied to the data. The results of the local dispersion analysis were coincide with those of the fractal dimension analyses.

We can consider the fractal dimension D, evaluated in the present work, as being the dimension of an attractor displayed in the 2-dimensional phase space because $D = 2$ for random noise: the dimension of the attractor in a phase space for random noise is equal to the dimension of the phase space where data are embedded. The fractal dimension evaluated in the present work has a scale dependence. In this respect, we can also infer that a fractal dimension of the attractor of $Z(t)$ in the phase space would have a scale dependence, as stated in section 1.

Acknowledgments

The content of this paper is a part of the Master Thesis of one of the authors (T.I.). We wish to thank Prof. S. Miyahara and Prof. O. Morita of Kyushu University and Prof. M. Takahashi of University of Tokyo for their helpful guidance and discussions. We also express our sincere thanks to Dr. J.-I. Yano of NCAR for his valuable comments and encouragement.

References

[1] C. Nicolis and G. Nicolis, Nature **311** (1984) 529.
[2] K. Fraedrich, J. Atmos. Sci. **43** (1986) 419.
[3] C. Essex, T. Lookman and M. A. H. Nerenberg, Nature **326** (1987) 64.
[4] A. A. Tsonis and J. B. Elsner, Nature **333** (1988) 545.
[5] H. W. Henderson and R. Wells, Adv. Geophys. **30** (Academic Press, New York, 1988) 205.
[6] P. Yang, D.-r. Lu, W. Li, B. Wu, S. Fukao, M. Yamamoto, T. Tsuda and S. Kato, Radio. Sci. **25** (1990) 1065.
[7] E. N. Lorenz, Nature **353** (1991) 241.
[8] X. Zeng and R. A. Pielke, J. Atmos. Sci. **49** (1992) 649.
[9] L. A. Smith, Phys. Lett. A **133** (1988) 283.
[10] M. A. H. Nerenberg and C. Essex, Phys. Rev. A **42** (1990) 7065.
[11] D. Ruelle, Proc. Roy. Soc. London. A **427** (1990) 241.
[12] J.-I. Yano and N. Nishi, J. Meteor. Soc. Japan **67** (1989) 771.

[13] T. Higuchi, Physica D **31** (1988) 277.
[14] T. C. Halsey, M. H. Jensen, L. P. Kadanoff, I. Procaccia, and B. I. Shraiman, Phys. Rev. A **33** (1986) 1141.
[15] L. F. Burlaga and L. W. Klein, J. Geophys. Res. **91** (1986) 347.
[16] M. L. Blackmon, J. Atmos. Sci. **33** (1976) 1607.
[17] J. Egger and H.-D. Schilling, J. Atmos. Sci. **40** (1983) 1073.
[18] J. Egger and H.-D. Schilling, J. Atmos. Sci. **41** (1984) 779.
[19] J. G. Charney, J. Meteorol. **4** (1949) 135.
[20] E. T. Eady, Tellus **1** (1949) 33.
[21] R. S. Lindzen, *Dynamics in atmospheric physics*. (Cambridge University Press, Cambridge, 1990).